JOURNAL OF Materials CHEMISTRY

XANES investigations and catalytic properties of coprecipitated AlF_3/MgF_2 phases

Ingolf Grohmann,[a] André Hess,[a] Erhard Kemnitz,*[a] Winfried Fentrup,[b] Wolfgang E. S. Unger,[c] Joe Wong,[d] Michael Rowen,[e] Takaho Tanaka[f] and Michael Fröba*[d,g]

[a]*Humboldt-Universität zu Berlin, Institut für Chemie, Hessische Str. 1-2, D-10115 Berlin, Germany*
[b]*Humboldt-Universität zu Berlin, Institut für Physik, EES, Invalidenstr. 110, D-10115 Berlin, Germany*
[c]*Bundesanstalt für Materialforschung und -prüfung, Labor VIII.23, Unter den Eichen 87, D-12205 Berlin, Germany*
[d]*Lawrence Livermore National Laboratory, University of California, Livermore, CA 94551, USA*
[e]*Stanford Synchrotron Radiation Laboratory, Stanford, CA 94309, USA*
[f]*National Institute for Research in Inorganic Materials, 1-1 Namiki, Tsukuba, Japan*
[g]*Universität Hamburg, Institut für Anorganische und Angewandte Chemie, Martin-Luther King Platz 6, D-20146 Hamburg, Germany*

Stepwise replacement of aluminium by magnesium in β-AlF_3 phases leads to considerable alterations in the structure and surface properties of the calcination products of co-precipitates. This is accompanied by significant changes in the catalytic activity for heterogeneous chlorine/fluorine exchange reactions. The maximum catalytic activity is reached between 10 and 20 atom% magnesium doping. Due to the decrease of the strength of Lewis acid sites with further increasing the Mg content, the catalytic activity is more and more diminished. The XRD patterns indicate a loss of crystallinity for β-AlF_3 with increasing Mg content. From Mg K-edge XANES and Al K-edge XANES spectra of Mg added β-AlF_3 phases one can conclude a partial incorporation of Mg into the β-AlF_3 lattice. Furthermore, a partial electron transfer from magnesium to the β-AlF_3 lattice resulting in an increased electron deficiency (increased Lewis acidity) at low Mg concentrations can be stated, a result which correlates well with the increased catalytic activity observed for co-precipitated phases with lower Mg contents. The insertion of Mg into the β-AlF_3 lattice is also supported by XPS studies on the same samples which show an increase of the modified Auger parameter for magnesium of about 0.4 eV, which indicates a change of the chemical environment of the ionized magnesium atom.

Introduction

Partially fluorinated aluminium oxides and aluminium fluorides are widely used as catalysts for heterogeneous fluorine-for-chlorine exchange reactions. One important application is their utilization in the synthesis of a new generation of freon alternatives, the chlorine free hydrofluorocarbons (HFCs).[1–6] As was shown previously,[4–10] the catalytic activity of the oxidic solid becomes increased due to its partial or complete fluorination. In the alumina system the metastable β-AlF_3 phase seems to be one of the most active phases.[8,9] It is well known from numerous catalyst systems that replacement of a metal by others can influence the catalytic activity to some extent. Therefore, attempts were undertaken to modify the catalytic activity of the β-AlF_3 phase by partial replacement with other metals, such as chromium and magnesium.[10] For instance, the partial replacement of Al by Mg resulted in enhanced catalytic activity at low magnesium concentrations. XRD analysis of the same samples gave not entirely clear information on the solid phases formed.

Consequently, in addition to the former catalytic tests, XANES measurements were carried out in order to describe the structural alterations as a result of stepwise introduction of magnesium in β-AlF_3. The results will be discussed with regard to the catalytic activity data of the relevant phases. The main results of additional XPS measurements are also considered.

Experimental

Preparation of the catalysts

The catalysts were synthesized by co-precipitation of α-$AlF_3 \cdot 3H_2O/MgF_2$ and subsequent calcination. In detail, basic aluminium acetate $Al(OH)(CH_3COO)_2$ was dissolved in 40 wt.% hydrofluoric acid. A solution of the agent to be used for co-precipitation was prepared by dissolving magnesium nitrate in ethanol. This solution was added to the first one. The co-precipitate was separated and calcined under argon flow (temperature programmed, maximum temperature: 420 °C). The sample powder was covered by an aluminium foil to establish a 'self-produced atmosphere'. The concentration of the metal to be added (Mg) is given in mol% of the total metal content of the solid. All sample notations refer to the cation concentrations of the initial solutions.

All samples were characterized by X-ray powder diffraction using an XRD 7 Seiffert-FPM (Freiburg, Germany; Cu-Kα radiation). The specific surface areas of the samples were determined using a ASAP 2000 system (Micromeritics) based on the nitrogen BET method (maximum experimental error ±1%). TPD measurements were performed as described previously. Characteristic data for the samples under investigation are summarized in Table 1.

Temperature-programmed desorption

The temperature-programmed desorption of ammonia as the probe molecule was employed for the determination of the strength distribution of acid sites. An adsorption feed of 18 ml ammonia was fed to 0.5 g of the solid sample at 1000 °C (flow system, permanent nitrogen flow). After that, a temperature program was started (following the feed pulse for 5 min isothermally at 100 °C, programming at $7.5\ K\ min^{-1}$ up to 475 °C, total run time 55 min). An FTIR flow cell was used for detection of desorbed ammonia. Further details are given in ref. 9. Table 1 presents the amounts of desorbed ammonia per gram of catalyst with regard to the relevant desorption tem-

Table 1 Elemental composition, specific surface area (BET) and amount of desorbed ammonia (TPD region 325–400 °C) of various Mg replaced β-AlF_3 samples

sample notation	Mg/(Mg+Al) (precursors) (mol%)	specific surface area/m^2 g^{-1}	desorbed ammonia (TPD)/mmol g^{-1}
β-AlF_3	0	31	222
Mg3	3	33	230
Mg10	10	40	242
Mg20	20	42	235
Mg35	30	46	160
Mg50	50	45	135
MgF_2	100	57	137

perature region of 325–400 °C. Previous studies[9] have shown that this particular acid strength interval correlates with the catalytic activity.

Catalytic characterization

As the test reaction for the characterization of the catalytic activity of all modified β-AlF_3 samples the dismutation of CCl_2F_2 [eqn. (1)] was employed.

$$2\ CCl_2F_2 \rightarrow CCl_3F + CClF_3 \qquad (1)$$

The products undergo further dismutation reactions. In detail, a constant weight of 0.6 g of the catalyst was used in a flow reactor (nickel tube). A residence time of 2 s was set up by adjusting the appropriate gas flow. The samples were calcined under nitrogen flow at 400 °C for one hour and then subsequently treated with a CCl_2F_2 flow at 390 °C. The composition of the gas phase at the exit of the reactor was determined by gas chromatography (column: Poraplot u, i.d. 0.53 mm, length 25 m). The conversion of the starting substance CCl_2F_2 is given with an absolute experimental error which did not exceed $\pm 0.5\%$ conversion.

XPS measurements

XP spectra were taken by a VG Scientific ESCALAB 200X electron spectrometer. XPS and XAES narrow scan spectra were acquired at Al-Kα excitation (15 kV, 20 mA) in FRR mode (CRR 40). The spectrometer energy scale was calibrated employing the procedure and binding energy reference data recommended by Anthony and Seah.[11] The sample powders were prepared on standard VG sample stubs with the help of double-sided adhesive films. Before recording spectra, the samples were stored to degas for one night at 10^{-7} mbar within the extended preplock of the spectrometer. The vacuum within the spectrometer chamber during measurements was better than 10^{-8} mbar. XP spectral analysis was performed by peak fitting employing the procedures of the SCIENTA ESCA-300 data system.

XANES measurements

Mg XANES measurements were performed in the fluorescence yield (FY) mode using a fluorescence spectrometer with a high purity germanium detector at BESSY I (BESSY mbH, Berlin, Germany). The resolution of the monochromator at the Mg K-edge was about 1.0 eV. The spectrometer together with the main chamber of the experiment was installed at BESSY's KMC monochromator beamline (42.21) using beryl (1010) crystals. The first peak in the derivative spectrum of metallic Mg at 1303 eV was used for energy calibration of the KMC monochromator.

The Al K-edge X-ray absorption near edge structure (XANES) spectra were recorded at the Stanford Synchrotron Radiation Laboratory (SSRL) with the SPEAR storage ring operating at 3 GeV and 50–100 mA. JUMBO beam line 3-3 was used with a YB_{66} (400) double-crystal monochromator.[12,13] All spectra were collected at room temperature in a step-scanning mode (counting time: 2 s; step-size: 0.2 eV) by monitoring the total electron yield (TEY) with a channeltron detector. The resolution of the monochromator at the Al K-edge was about 1.0 eV.

In all cases, each edge was energetically calibrated with the help of the edge of the respective pure element (Mg K edge: 1404 eV; Al K-edge: 1559 eV). A pre-edge fit was applied and all spectra were normalized for atomic absorption.

Results and Discussion

All samples investigated in this study were checked regarding their catalytic activity for disproportionation reactions of difluorodichloromethane. As has already been shown, the disproportionation reaction following eqn. (1) occurs predominantly at Lewis acidic surface sites.[10] Replacing aluminium by magnesium results in an alteration of the Lewis acidity of the catalyst. The catalytic activity of the calcined samples passes, as is shown by Fig. 1, through a maximum observed at the 10% magnesium containing sample. Due to the decrease of the strength of Lewis acid sites with further increasing the Mg content, the catalytic activity diminishes further. At 50% and higher Mg contents the strength of Lewis acid sites is no longer sufficiently enough to catalyze the test reaction [eqn. (1)].

The XRD patterns (*cf.* Fig. 2) of the calcined samples indicate a loss of crystallinity for β-AlF_3 with increasing Mg content. With further increase of the Mg content, the reflections of MgF_2 become more and more visible. A slight increase of the β-AlF_3 lattice constant, particularly for the 50% sample, was detected for the co-precipitated samples. Since the crystallinity of these catalysts was quite low, XANES spectroscopy was applied in order to monitor the effects of Mg insertion in more detail.

Fig. 3 shows the normalized Mg K-edge XANES spectra of Mg substituted β-AlF_3 and pure MgF_2 samples. With increasing aluminium content an increase in intensity of the white line (first peak) and a small positive shift of the K-edge of about 0.3 eV is observed. In addition, a change in the near-edge structure above 1320 eV occurs, a region which is mainly determined by multiple scattering effects within the medium range structure. All these changes can be explained by a partial insertion of Mg into the β-AlF_3 lattice.

The white line corresponds to an s–p transition. Due to the lower electronegativity of magnesium with regard to aluminium the electron density of the Mg 2p orbitals decreases with increasing aluminium content. This causes more vacancies in

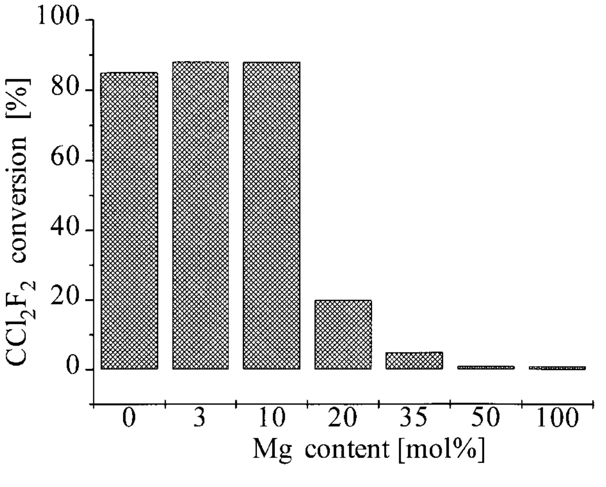

Fig. 1 Disproportionation activity of β-AlF_3 with Mg cations successively added

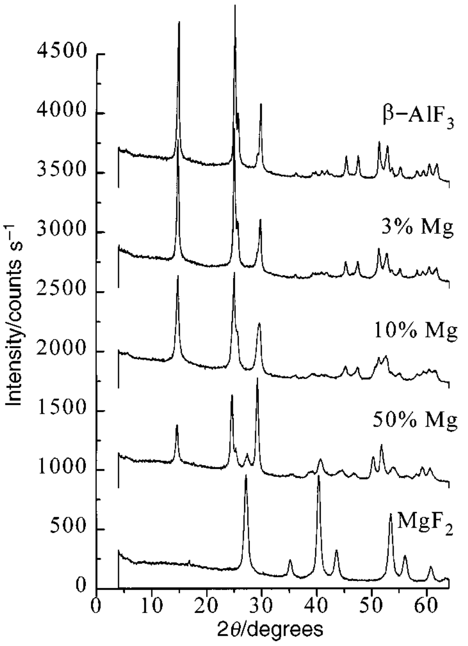

Fig. 2 Powder diffraction patterns of β-AlF$_3$ with Mg cations successively added

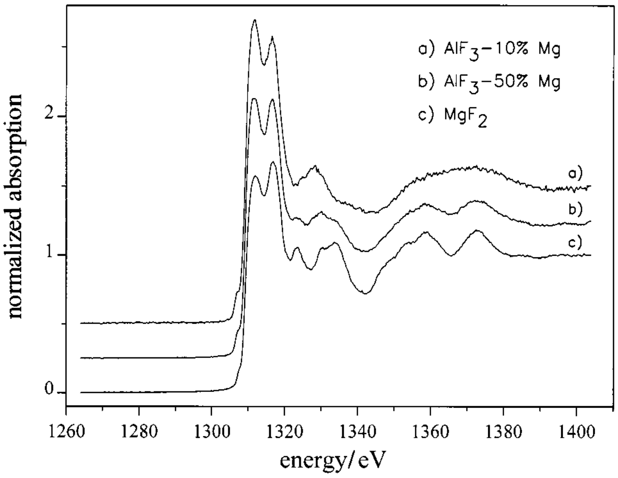

Fig. 3 Normalized FY K-edge XANES spectra of magnesium in MgF$_2$ and different calcined Al/Mg fluoride co-precipitates. A to E denote the sharp resonant absorption features for Mg in MgF$_2$.

the p-orbitals of magnesium and increases the s–p transition probability which consequently results in a higher intensity of the white line. In an analogous manner the increase in intensity of the pre-edge peaks, arising from other bound state transitions of inner atomic electrons, can be explained. The decreased screening of the Mg nucleus by the valence electrons also increases the binding energy of the Mg 1s electron and therefore the edge energy. The changes of the peak structure in the energy range between 1320 eV and 1340 eV can be attributed to changes in the medium range order. The shift of the peaks towards lower energies (E) with increasing Al content indicates an increase in the inter-atomic distances (R) around the Mg absorber atom according to the relationship $E = 151/R^2$.[14] Furthermore, peak structures above 1340 eV became very broad indicating a loss of ordering.

For comparison, in Fig. 4 the normalized Al K-edge XANES spectra of β-AlF$_3$ and Mg added AlF$_3$ samples are plotted. In contrast to the corresponding magnesium spectra a decrease of the intensity of the white line with respect to the pure substance is observed at higher Mg concentrations whereas, especially at low Mg contents (up to 10%), the intensity remains constant. The insertion of Mg into the β-AlF$_3$ lattice seems to be without any influence at low concentrations but it increases the electron density of the Al 2p orbitals at higher contents. This results in a decreased s–p transition probability and consequently in a lower intensity of the white line. The β-AlF$_3$ structure remains nearly unchanged, although a slightly increased distortion with increasing Mg content can be observed. Here the leveling of the XANES structures is in the range between 1580 and 1590 eV, which represents an energy range which is determined by the medium range order.[15] Although the EXAFS region could provide some more detailed information on the changing local structures of the metal atoms with respect to changes in the Mg : Al ratios, this was impossible in the case of these samples for several reasons. Firstly, the signal to background ratio in the EXAFS region is generally not that good and particularly in these measurements it is too noisy to allow detailed conclusions on the electronic aspects of the metal environments. Secondly, magnesium and aluminium are neighbouring elements in the Periodic Table and consequently too similar to be differentiated under the measuring conditions used.

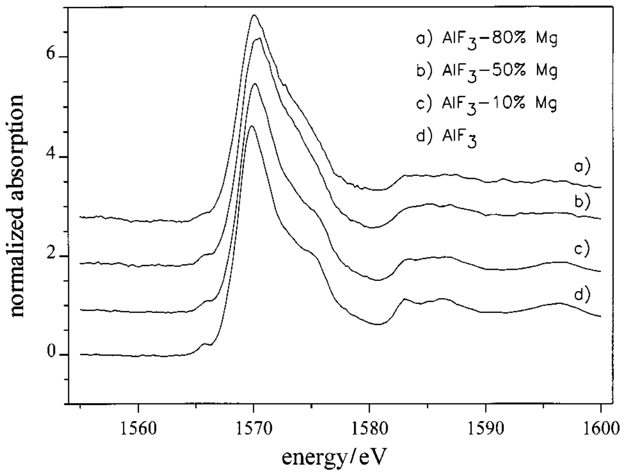

Fig. 4 Normalized TEY K-edge XANES spectra of aluminium in β-AlF$_3$ and different calcined Al/Mg fluoride co-precipitates

However, from XRD and XANES one can conclude a successive substitution of aluminium by magnesium in the β-AlF$_3$ lattice at least at lower Mg concentrations. If the magnesium content exceeds a concentration of about 20% relative to Al, MgF$_2$ becomes more and more visible as an additional phase. As long as magnesium is completely incorporated in the β-AlF$_3$ lattice increased catalytic activity can be observed. The segregation of pure MgF$_2$ is the reason for fundamental changes in the catalytic behaviour of the samples (*cf.* Fig. 1). On the basis of XANES measurements it can be stated that low concentrations of magnesium substitutions provide an increased electron affinity (Lewis acidity) of the Mg sites whereas at the same time the valence electron density of the Al sites remains at least unchanged. Obviously, that finally results in an increased integral Lewis acidity and, therefore, in a higher catalytic activity.

The insertion of Mg into the β-AlF$_3$ lattice is also supported by XPS studies on the same samples which show an increase of the modified Auger parameter for magnesium of about 0.4 eV (see Table 2). This indicates a change of the chemical environment of the ionized magnesium atom. Additionally performed Au $4f_{2/7}$ referenced XPS measurements for the same catalyst system[16] are in agreement with the conclusions drawn from XANES investigations reported in this paper. It was

Table 2 Modified Auger parameter α' evaluated with the kinetic energy of the KLL Auger transition and the binding energy of the 1 s photoelectrons of magnesium

sample	Mg α'/eV
MgF_2	2483.1
β-AlF_3/50% Mg	2482.8
β-AlF_3/10% Mg	2482.7
β-AlF_3/3% Mg	2482.6

Table 3 Surface stochiometry (without H) of different β-AlF_3 samples with Al sucessively replaced by Mg

sample	nominal bulk stochiometry	surface stochiometry (without H)
Mg3	$Al_{0.97}Mg_{0.03}F_{2.97}$	$Al_{0.95}Mg_{0.05}F_{2.25}O_{0.14}$
Mg10	$Al_{0.90}Mg_{0.10}F_{2.90}$	$Al_{0.89}Mg_{0.11}F_{2.18}O_{0.22}$
Mg20	$Al_{0.80}Mg_{0.20}F_{2.80}$	$Al_{0.76}Mg_{0.24}F_{2.08}O_{0.18}$
Mg35	$Al_{0.65}Mg_{0.35}F_{2.65}$	$Al_{0.52}Mg_{0.48}F_{2.03}O_{0.18}$
Mg50	$Al_{0.50}Mg_{0.50}F_{2.50}$	$Al_{0.43}Mg_{0.57}F_{1.89}O_{0.19}$

proved by XPS that both the Mg—F and the Al—F binding energies increase with stepwise Mg replacement. More important, and, surprising at the same time, is that the relaxation energy (Mg 1s, Mg 2p) decreases from Mg3 to Mg20. Further, it increases again to Mg50. Obviously, samples with higher Mg contents ($\geqslant$20% Mg) possess the same complex relaxation behavior as pure MgF_2, which suggests that small MgF_2-like crystallites already exist in Mg35 and Mg50.

On the basis of this experimental evidence we conclude an incorporation of Mg into the Al sublattice of β-AlF_3 at lower Mg concentrations, which is also in accordance with the slightly decreased middle range order analyzed by XANES. The arrangement of the AlF_6 octahedra linkage in the HTB structure of β-AlF_3 is shown in Fig. 5. A possible surface structure of β-MF_3 phases was assumed for M = Al[10] and M = Cr[17] consisting of a buckled surface with partly unsaturated M^{3+} cations on the top being able to act as accessible Lewis acid sites on the surface. A partial replacement of Al by Mg most probably produces vacancies in the anion sublattice and, consequently, gives rise to an increased number of vacancies in the surface too, resulting in increased surface activity due to a better accessibility of the metal cations by Lewis base (in this case the halogen atoms of a haloalkane molecule).

An alternative model to explain the observed structural and catalytic changes as a function of the Mg to Al ratio in β-AlF_3 is based on our XPS results, discussed above. Even from these XPS data below a critical Mg content ($\leqslant$20% Mg) there is some evidence for the formation of smaller, 'cluster-like' Mg_xF_y units along the parallel hexagonal channels in the β-AlF_3 framework, which, however, are still too small to be considered as a separated MgF_2 phase. Thus, finite domains of MgF_6 octahedra could be formed, which are statistically separated from each other. Therefore they should be regarded as embedded 'clusters' but not as a separated phase. Consequently, HTB-related phases are known only for compositions like $M^{II}M^{III}F_5$ or $M^{I}M^{II}M^{III}F_6$, where M^{I} in particular, but also M^{II}, represent large cations due to the large cross-section of the tunnels.[18] For example, caesium compounds $Cs_yM^{II}_yM^{III}_{2-y}F_6$ are formed in a HTB structure type at low values of y and in a pyrochlore structure type at high values of y. The intermediate range is a two-phase domain.[19] On the basis of these structural and stability relationships it is understandable that (i) in the binary phase system AlF_3–MgF_2 pure stochiometric ternary fluorides are not formed and (ii) even in the case of a partial incorporation of MgF_2 at lower concentrations a further increase of the Mg content in β-AlF_3 ($\geqslant$20% Mg) results in a segregation of pure MgF_2, which probably results in increased surface coverage by catalytically inactive MgF_2. In fact, a comparison of the expected bulk stochiometry with the XPS-detected surface stochiometry, as shown in Table 3, confirms this conclusion. Especially for samples above Mg20 a higher content of Mg was found in comparison with the nominal bulk stochiometry.

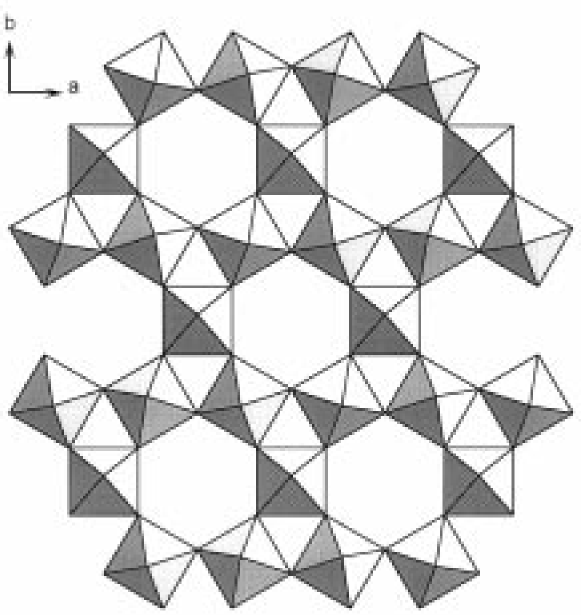

Fig. 5 Octahedra connectivity in the hexagonal tungsten bronze structure of β-AlF_3

Thanks are due to the Lawrence Livermore National Laboratory and the Chemical Division of the U.S. Department of Energy (DOE) and Dr. W. Braun (BESSY mbH, Berlin) for supporting XANES measurements at the Stanford Synchrotron Radiation Laboratory (SSRL) and at BESSY, respectively. E. K. thanks the Deutsche Forschungsgemeinschaft (DFG, Ke-489/7-1), the Fonds der Chemischen Industrie (FCI) and Du Pont de Nemours for financial support. M. F. thanks the Alexander von Humboldt Foundation for a Feodor Lynen Research Fellowship.

References

1 S. Brunet, B. Requieme, E. Matouba, J. Barrault and M. Blanchard, *J. Catal.*, 1995, **152**, 70.
2 T. H. Ballinger and J. T. Yates, *J. Phys. Chem.*, 1992, **96**, 1417.
3 T. H. Ballinger, R. S. Smith, S. D. Colson and J. T. Yates, *Langmuir*, 1992, **8**, 2473.
4 J. Thomson, G. Webb and J. M. Winfield, *J. Chem. Soc., Chem. Commun.*, 1991, 323.
5 J. Thomson, G. Webb, J. M. Winfield, D. Bonniface, C. Shortman and N. Winterton, *Appl. Catal. Ser. A*, 1993, **97**, 67.
6 A. Hess and E. Kemnitz, *J. Fluorine Chem.*, 1995, **74**, 27.
7 A. Kohne and E. Kemnitz, *J. Fluorine Chem.*, 1995, **75**, 103.
8 A. Hess, E. Kemnitz, A. Lippitz, W. E. S. Unger and D. H. Menz, *J. Catal.*, 1994, **148**, 270.
9 A. Hess and E. Kemnitz, *J. Catal.*, 1994, **149**, 449.
10 E. Kemnitz, A. Hess, G. Rother and S. Troyanov, *J. Catal.*, 1996, **159**, 332.
11 M. T. Anthony and M. P. Seah, *Surf. Interface Anal.*, 1984, **6**, 95.
12 J. Wong, G. Shimkaveg, W. Goldstein, M. Eckart, T. Tanaka, Z. U. Rek and H. Tompkins, *Nucl. Instrum. Methods A*, 1990, **291**, 243.
13 J. Wong, G. N. George, I. J. Pickering, Z. U. Rek, M. Rowen, T. Tanaka, G. H. Via, B. DeVries, D. E. W. Vaughan and G. E. Brown, Jr., *Solid State Commun.*, 1994, **92**, 559.
14 C. R. Natoli, *Proc. 3rd EXAFS Conf.* (*XAFS3*), *Stanford, USA*, in *EXAFS and Near-Edge Structure III*, ed. K. O. Hodgson, Springer Proc. Phys. 2, Springer-Verlag, New York, 1984, pp. 38–42.

15 M. Fröba, P. Behrens, J. Wong, G. Engelhardt, Ch. Haggenmüller, G. van de Goor, M. Rowen, T. Tanaka and W. Schwieger, *Mater. Res. Soc. Symp. Proc.*, 1995, **317**, 99.
16 O. Böse, E. Kemnitz, A. Lippitz and W. E. S. Unger, *Appl. Surf. Sci.*, in press.
17 E. Kemnitz, A. Kohne, I. Grohmann, A. Lippitz and W. E. S. Unger, *J. Catal.*, 1996, **159**, 270.
18 D. Babel and A. Tressaud, *Crystal Chemistry of Fluorides*, in *Inorganic Solid Fluorides*, ed. P. Hagenmuller, Academic Press Inc., New York, 1985, pp. 77–203.
19 D. Babel, F. Binder and G. Pausewang *Z. Naturforsch. B: Anorg. Chem., Org. Chem.*, 1973, **28**, 213.

Paper 8/01131A; *Received* 9*th February*, 1998